

Fe[4,4'-Bis(methylphosphonate)-2,2'-bipyridine]<sub>2</sub>(CN)<sub>2</sub> Based Photosensitizers

Angela Suzanne Peters

Department of Energy: Energy Research Undergraduate Laboratory Fellowship Program

Wartburg College – Waverly, Iowa 50677

National Renewable Energy Laboratory

Golden, CO 80401

August 10, 2000

Prepared in partial fulfillment of the requirements of the Department of Energy: Energy Research Undergraduate Laboratory Fellowship Program under the direction of Suzanne Ferrere in the Basic Sciences Division at the National Renewable Energy Laboratory.

Participant: \_\_\_\_\_

Signature

Research Advisor: \_\_\_\_\_

Signature



### Abstract

Fe[4,4'-Bis(methylphosphonate)-2,2'-bipyridine]<sub>2</sub>(CN)<sub>2</sub> Based Photosensitizers. ANGELA SUZANNE PETERS (Wartburg College, Waverly, Iowa 50677) S. Ferrere (National Renewable Energy Laboratory, Golden, Colorado 80401).

Iron(II) bipyridine based photosensitizing dyes have recently gained attention. This focus was spurred by the successful conclusion in the ability for Fe(4,4'-dicarboxylic acid-2,2'-bipyridine)<sub>2</sub>(CN)<sub>2</sub> to sensitize nanocrystalline titanium dioxide (Ferrere et al., 1998). In the past, Ruthenium bipyridines have been an extensively researched dye-base used in photochemical systems. On the other hand, little has been done in the research and investigation of apparent iron analogues. Therefore, the focus of this research is to study one of these iron-based dye molecules. The synthesis, spectral characteristics, and electrochemical behavior of Fe(4,4-Bis(methylphosphonate)-2,2'-bipyridine)<sub>2</sub>(CN)<sub>2</sub> is reported in the following dialog.

#### Research Category (Please Circle)

ERULF:    Physics    Chemistry    Biology    Engineering    Computer Science  
Other \_\_\_\_\_  
CCI:    Biotechnology    Environmental Science    Computing

#### TYPE ALL INFORMATION CORRECTLY AND COMPLETELY

School Author Attends	_____	Wartburg College
DOE National Laboratory Attended	_____	National Renewable Energy
Laboratory	_____	
Mentor's	Name: _____	Suzanne Ferrere
	Phone: _____	(303) 384-6686
	E-mail: _____	suzanne_ferrere@nrel.gov

Author's Name:	_____	Angela S. Peters
Mailing Address:	_____	9743 Sylvan Dr.
City/State/ZIP:	_____	Janesville, IA 50647
Phone:	_____	(319) 987-2131
E-mail Address:	_____	petersan@wartburg.edu

Is this being submitted for publication?: Yes No  
DOE Program: ERULF CCI PST (circle one only)

## INTRODUCTION

The idea of transforming sunlight into electricity was first recognized with Becquerel's 1839 observation of the existence of a light-dependent voltage between electrodes immersed in an electrolyte. This was termed the photovoltaic effect. However, it was not until 1941 that the first photovoltaic structure was developed that converted light to electricity with a reasonable efficiency. This major advancement was found in the development of the silicon cell. The first application of this cell was initiated in 1958 with the installation of such technology in spacecraft. Finally, in the 1970s, solar cells were beginning to be seen in a more practical, terrestrial sense. By the conclusion of the 1970s, the terrestrial applications of solar cells far out-weighed those found in space. (Green, 1982)

In the 1980s, the field of solar cell development began to intensify. This was a direct result of the cells' increased interest and decreased cost. Since then, research associated with his field has taken several different paths. The path that I spent my summer on was that of dye-sensitized solar cells.

When discussing dye-sensitized solar cells, it is first vital to look at the overall construction of the system. The cell is constructed of three main components: photoanode, cathode and electrolyte solution. The photoanode is constructed of a 10-20  $\mu\text{m}$  thick nanocrystalline film consisting of titanium dioxide ( $\text{TiO}_2$ ) particles. These particles are attached to a transparent conducting glass substrate. Adsorbed to the  $\text{TiO}_2$  film is a monolayer of dye molecules. The pores of the nanocrystalline film are filled with a liquid electrolyte solution consisting of iodide/triiodide redox coupled in a non-aqueous electrolyte. One such solution is acetonitrile. The cathode is a transparent conducting glass

substrate that behaves as the counter electrode in the system. This substrate is then placed over the nanocrystalline  $\text{TiO}_2$ , and the edges are sealed.

It is also important to understand how a solar cell works. When light from the sun hits the dye molecules, the cell is excited and dye molecules inject electrons into the conduction band of the  $\text{TiO}_2$ . The injected electrons then permeate through the nanocrystalline film with little energy loss and are collected at the glass substrate. After the electrons complete this external circuit they are able to deliver power to the load. The electrons then re-enter the cell at the counter electrode. Here they reduce the triiodide to iodide and diffuse into the pores of the  $\text{TiO}_2$  to reduce the photo-oxidized dye back to its original state. It is now that the electrons have completed the circle. (see Figure 1)

The two most significant components found in dye-sensitized solar cells are the nanocrystalline film and the dye itself. In recent years, scientists in the field have heavily researched both of these components.

The first of these components, the porous nanostructured film, serves as the semiconductor in the system. Currently,  $\text{TiO}_2$  is the preferred semiconductor material being used (Kalyanasundaram, 1999). In the 1980s, Lausanne was the first to investigate nanocrystalline  $\text{TiO}_2$  as a substrate for photosensitization. Having an effective band gap of 3.2 eV,  $\text{TiO}_2$  is insensitive to visible light (Grätzel et al., 1994). However, it is cheap, widely available, non-toxic, able to be photosensitized by a wide range of dyes, and fully stable in electrolytes under illumination. It is also found in numerous materials on the market today. Some of these include the white pigment in paint and paper as well as an abrasive in toothpaste.

The key ingredient in the cell is the dye. Without this, the cell is unable to use the sun's light at all. The dye used must contain three vital features. First, the dye must be capable of absorbing light over a relatively wide spectral range. It must also be able to inject an electron from its excited state into the semiconductor's conduction band. And finally, the dye must display an excellent level of stability that will allow for the completion of hundreds of thousands of excitation-oxidation-reduction cycles to be achieved over the required operational lifetime of twenty years (Kalyanasundaram, 1999).

In 1978, Chen, Deb, and Witzke were the first to demonstrate the use of a dye-sensitized cell with N-methylphenazium serving as the dye. This dye extended the spectral response of TiO<sub>2</sub> into the 500-nm region (Ellingson et al., 1998). The conversion efficiency of this first attempt was relatively low and the stability of the dye was questioned. As a result of this, the dye-sensitized cell's application to everyday life seemed questionable.

Significant advancement was achieved in 1991 with the work conducted by Grätzel and O'Regan. This research found that ruthenium (Ru<sup>II</sup>)-complex dyes displayed both increased efficiency and stability. Today, the standard dye used is Ru<sup>II</sup>(4,4'-dicarboxy-2,2'-bipyridine)<sub>2</sub>(NCS)<sub>2</sub> (see Figure 2). Under standard solar conditions, this complex demonstrates conversion efficiencies in the 7-10% range (Ellingson et al., 1998). Since this time, the research and development of ruthenium-based dyes has seen a great amount of expansion.

Although ruthenium-based dye molecules have been studied in depth, their iron-based counterparts still lack a significant amount of research focus. Ferrere and Gregg reported the first efficient use of an iron (Fe<sup>II</sup>) bipyridyl complex in a photoconversion theme (Ferrere et al., 1998). The complex studied was Fe<sup>II</sup>(4,4'-dicarboxy-2,2'-

bipyridine)<sub>2</sub>(CN)<sub>2</sub> (see Figure 3). The results broadened the field of dyes considered as photosensitizers. This particular iron-based dye shows a unique “band selective” sensitization which effectively sensitizes TiO<sub>2</sub> from only one of its two absorption bands. However, photochemical applications of iron-bipyridyl complexes were originally not studied in depth because of their low lying ligand field (LF) states which deactivate the initially populated metal-to-ligand charge-transfer (MLCT) states. This results in extremely short-lived MLCT lifetimes (Ferrere et al., 1998). Hannappel, Ellingson, and Tachibana were each able to combat this initial doubt by demonstrating that the excited state electron injection from adsorbed dyes into the nanocrystalline TiO<sub>2</sub> could occur within several hundred femtoseconds. Additionally, a greater level of efficiency from the higher energy MLCT absorbance band than the lower energy MLCT was surprisingly found as a result of the dye’s “band selective” characteristic (Ferrere, 1998).

So then, the question: what are the true benefits to using an iron-based dye. Iron is the most abundant transition metal on earth. It is available from numerous recycled materials and its bipyridyl complexes are recyclable. Since the colors obtained from iron dyes extend further into the red, they complement their ruthenium analogues very well. Additionally, iron is a cheaper alternative to ruthenium.

My work at the National Renewable Energy Laboratory this summer was centered on the development of the following iron-based dye molecule: Fe<sup>II</sup>(4,4'-Bis(methylphosphonate)-2,2'-bipyridine)<sub>2</sub>(CN)<sub>2</sub> (see Figure 4). In rest of this paper, I will address the synthesis, spectral characteristics, and electrochemical behavior of this iron-based dye.

## EXPERIMENTAL

**Materials and Methods.** All reagents were commercially available purest grade and obtained from Aldrich Chemical Company. A Hewlett Packard 8543 UV-VIS Spectrophotometer was used to measure absorbance spectra. A Thermolyne 48000 Furnace was used during the baking process of the TiO<sub>2</sub> plates. The ActSpec.Appl. v A1.4\* of Lab View 4 was used to obtain absorbed photon-to-current efficiency vs wavelength data.

**Preparation of Ligands. 4,4'-dibromomethyl-2,2'-bipyridine** (see Figure 5) was prepared from 4.77 g of 4,4'-dimethyl-2,2'-bipyridine, 9.54 g of N-bromosuccinimide, and approximately 150 mL of carbon tetrachloride according to Gould (Gould, 1991). 8.86 g of 4,4'-dibromomethyl-2,2'-bipyridine were obtained which gives a yield of 5.44 percent.

NMR ( $\delta$  from TMS, D<sub>2</sub>O):  $\delta$  4.48 (s, H 2),  $\delta$  7.46 (q, H 1),  $\delta$  8.48 (q, H 1),  $\delta$  8.71 (q, H 1).

**4,4'-Bis(diethyl methylphosphonate)-2,2'-bipyridine** (see Figure 6) was prepared from 481.5 mg of 4,4'-dibromomethyl-2,2'-bipyridine and an excess amount of triethyl phosphite according to Hupp (Hupp, 1996).

**Preparation of Fe<sup>II</sup>(4,4'-Bis(methylphosphonate)-2,2'-bipyridine)<sub>2</sub>(CN)<sub>2</sub>.** Fe<sup>II</sup>(4,4'-Bis(methylphosphonate)-2,2'-bipyridine)<sub>2</sub>(CN)<sub>2</sub> was prepared by a variation of the process used by Ferrere and Gregg to produce Fe<sup>II</sup>(2,2'-bipyridine-4,4'-dicarboxylic acid)<sub>2</sub>(CN)<sub>2</sub> (Ferrere et al., 1998). 4,4'-Bis(diethyl methylphosphonate)-2,2'-bipyridine was refluxed in an excess amount of 6 M hydrochloric acid for approximately four hours. The pH of the solution was then raised to 6.5 with the addition of tetrabutyl ammonium hydroxide. Unwanted products were extracted from the solution through a separatory funnel by the addition of methylene chloride. The solution was then rotovapped as dry as possible but remained an oil despite several attempts at purification with methanol. The preparation

process was continued although the amount of reactant was uncertain. Therefore, it is impossible to determine the percent yield of the final product. To continue, the hydrolyzed product was dissolved in approximately 10 mL of water. Then an excess amount of the iron(II) salt,  $(\text{NH}_4)_2\text{Fe}(\text{SO}_4)_2 \cdot 6\text{H}_2\text{O}$ , was added. The solution was heated to boiling at which time 334 mgs of sodium cyanide dissolved in water was added. The solution was allowed to boil for approximately 15 minutes. During this heating cycle, the solution first turned to a purplish/red color and proceeded to red. After cooling to room temperature, the pH was lowered to approximately 3.4 by the addition of 0.005M sulfuric acid. Upon acidification, the solution turned purple. It was then rotovapped. Another oil was formed. However, with the addition of methanol, a precipitate formed. The filtrate was collected and purified on a sephadex column using methanol as the eluent. UV-VIS Spectrum was obtained and displayed the relative absorbance for the dye at approximately 543 nm (see Figure 7).

**Preparation of  $\text{TiO}_2$  coated conductive glass.** The nanocrystalline  $\text{TiO}_2$  film was applied to the conductive glass according to Ellingson et al. (Asbury et al., 1998).

**Adsorption of  $\text{Fe}^{\text{II}}(4,4'\text{-Bis(methylphosphonate)-2,2'\text{-bipyridine})}_2(\text{CN})_2$  onto  $\text{TiO}_2$  coated conductive glass.** The adsorption of the dye onto the  $\text{TiO}_2$  coated conductive glass plates was achieved by simply soaking the plates in the dye solution ( $\text{Fe}^{\text{II}}(4,4'\text{-Bis(methylphosphonate)-2,2'\text{-bipyridine})}_2(\text{CN})_2$  dissolved in a small amount of methanol) overnight.

## RESULTS

Six iron-sensitized solar cells were constructed using the methods detailed previously in this paper. Labels A, B, C, D, E, and F were given to the cells. Three measurements were then taken of each of the cells: Current vs Voltage (see Figure 7A – 7F), Absorbance, and Incident Photon Conversion to Electrons (IPCE). The Absorbance and IPCE data were compared on the same graphs (see Figure 8A – 8F).

From the data found in Figures 7A – 7F, it is seen that the maximum current for all of the cells is in the range of 45 to 50  $\mu\text{A}/\text{cm}^2$ . Cell A (Figure 7A) seems to be the most responsive. Past publications show  $\text{Fe}^{\text{II}}(2,2'\text{-bipyridine-4,4'-dicarboxylic acid})_2(\text{CN})_2$  to peak around 300  $\mu\text{A}/\text{cm}^2$  (Ferrere et al., 1998).

When looking at Figures 8A through 8F, it is first important to be able to interpret the data correctly. For clarification purposes, IPCE can be more simply thought of as the number of excited electrons in the system. In the wavelength range just below 450 nm, the  $\text{TiO}_2$  may still be absorbing; therefore, we disregard this area of the graph. Also, any sharp peaks found in the high wavelengths are quite possible random noise responses (see Figures 8A, 8C, and 8D). These peaks can also be disregarded. With all of this said, it makes sense that both Absorbance and the IPCE of the cells maximize at approximately the same wavelength of light. This should result, because the cell should prove most responsive in the wavelength region that it best absorbs light from the sun. In this case, the wavelength is around 480 nm.

## CONCLUSIONS

From the data shown in Figures 7 and 8, it is obvious that the  $\text{Fe}^{\text{II}}(4,4'$ -Bis(methylphosphonate)-2,2'-bipyridine) $_2(\text{CN})_2$  solar cell produced does in fact work. However, the efficiency of the cell is significantly less than that produced by the  $\text{Fe}^{\text{II}}(2,2'$ -bipyridine-4,4'-dicarboxylic acid) $_2(\text{CN})_2$  (Ferrere et al., 1998). The dye produced here obtains a maximum current around  $50 \mu\text{A}/\text{cm}_2$ , while the published dye reaches a maximum at a approximately  $300 \mu\text{A}/\text{cm}_2$  (Ferrere et al., 1998). One would expect that, since both are iron-based dyes, the efficiency levels would be comparable. A possible explanation for the difference is the distance of adsorption to  $\text{TiO}_2$  from the metal ligand. In the  $\text{Fe}^{\text{II}}(4,4'$ -Bis(methylphosphonate)-2,2'-bipyridine) $_2(\text{CN})_2$  dye, an extra carbon group is found between the iron-bipyridial ligand and the phosphonic acid adsorption point. This may account in the large difference between the two dyes. However, further research should be conducted on this note. It is important to now begin determining the exact effects that distance of adsorption to  $\text{TiO}_2$  from the metal ligand has on the efficiency of such solar cells.

Additionally, the preparation and exploration of iron(II)-based sensitizers should continue in the future. Two suggestions for the direction of this continuation are as follows. First, the effectiveness and efficiencies of various iron(II)-based dyes should be compared to determine the best characteristics. Also, it will be important to determine the role of the adsorptive properties of the dyes to ensure the best possible features.

## ACKNOWLEDGEMENTS

First, I would like to thank those individuals who were blessed with my shining face on a nearly daily occurrence. Thanks a million to my mentor, Suzanne Ferrere, who made my experience unbeatable. Also, thanks to Brian Gregg and Clark Fields for their company in the lab.

Secondly, thank you to the entire staff in the Basic Sciences Department of the National Renewable Energy Laboratory in Golden, Colorado. Special thanks to Inger Jafari for always greeting me with a smile and Jeff Blackburn for enlightening me in the cubicle.

Finally, thanks to the Department of Energy for creating the Energy Research Undergraduate Laboratory Fellowship (ERULF) Program. Especially, thanks to Linda Lung, Robi Robichaud, and John Sepich for all of their support and influence.

The research described in this paper was conducted in the Basic Sciences Division at the National Renewable Energy Laboratory in Golden, Colorado. My work was made possible through the ERULF Program sponsored by the United States Department of Energy.

## REFERENCES

Asbury, J. B., Ellingson, R. J., Ferrere, S., Ghosh, H. N., Lian, T., Nozik, A. J., Sprague, J. R. (1998). Dynamics of electron injection in nanocrystalline titanium dioxide films sensitized with [Ru(4,4'-dicarboxy-2,2'-bipyridine)<sub>2</sub>(NCS)<sub>2</sub>] by infrared transient absorption. Journal of Physical Chemistry B, v 102, 6455-6458.

Ellingson, R., Ferrere, S., Frank, B. A., Gregg, B. A., Nozik, A. J., Park, N., Schlichthörl, G. (1998). Photochemical solar cells based on dye-sensitization of

nanocrystalline TiO<sub>2</sub>. 2<sup>nd</sup> World Conference and Exhibition on Photovoltaic Solar Energy Conversion: Vienna, Austria, July 6-10, 1998.

Ferrere, S. & Gregg, B. (1998). Photosensitization of TiO<sub>2</sub> by [Fe<sup>II</sup>(2,2'-bipyridine-4,4'-dicarboxylic acid)<sub>2</sub>(CN)<sub>2</sub>]: Band selective electron injection from ultra-short-lived excited states. Journal of the American Chemical Society, v120, 843-844.

Gould, S., Meyer, T. J., Strouse, G. F., & Sullivan, B. P. (1991). Formation of thin polymeric films by electropolymerization. Reduction of metal complexes containing bromomethyl-substituted derivatives of 2,2'-bipyridine. Inorganic Chemistry, v30, 2942-2949.

Grätzel, M., & McEvoy, A. J. (1994). Sensitization in photochemistry and photovoltaics. Solar Energy Materials and Solar Cells, v32, 221-227.

Green, M. A. (1982). Solar Cells: Operating principles, technology, and system applications. Englewood Cliffs, N.J.: Prentice-Hall, Inc.

Hupp, J. T., Yan, S. G. (1996). Semiconductor-based interfacial electron-transfer reactivity: Decoupling kinetics from pH-dependent band energetics in a dye-sensitized titanium dioxide/aqueous solution system. The Journal of Physical Chemistry, v100, 6867-6870.

Kalyanasundaram, K. (February 2, 1999). A new type of solar cell based on sensitized, nanocrystalline semiconducting oxide films [online]. Available: <http://dcwww.epfl.ch/lpi/solarcellE.html>. (August 7, 2000)

## FIGURES

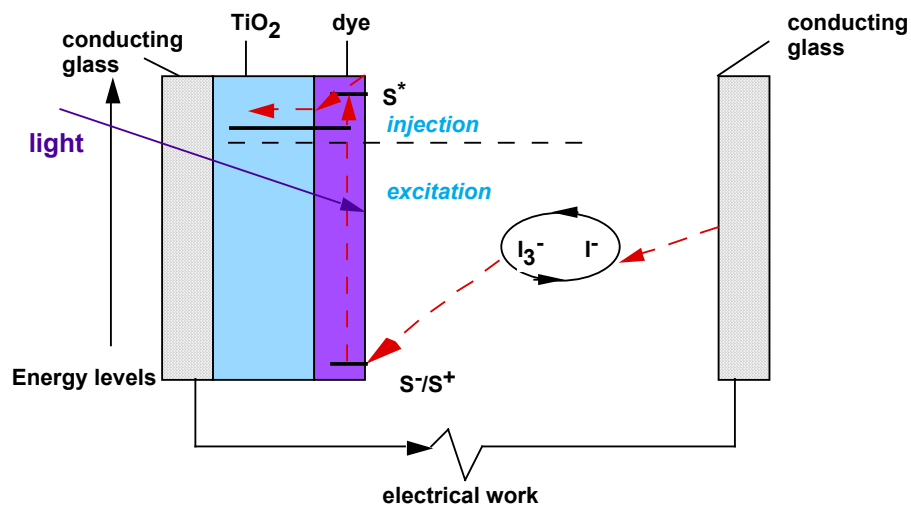


Figure 1: Structure of Dye-Sensitized Solar Cell.

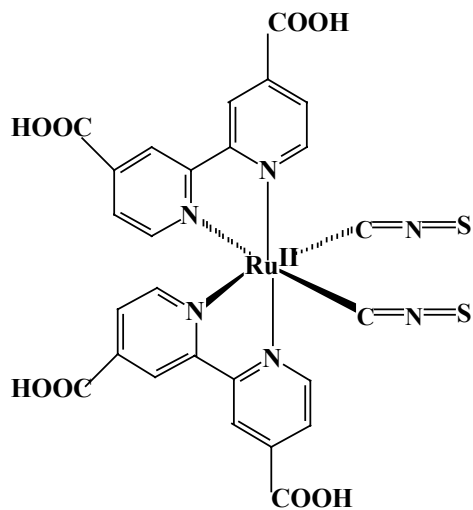


Figure 2: Molecular Structure of Ru<sup>II</sup>(4,4'-dicarboxy-2,2'-bipyridine)<sub>2</sub>(NCS)<sub>2</sub>.

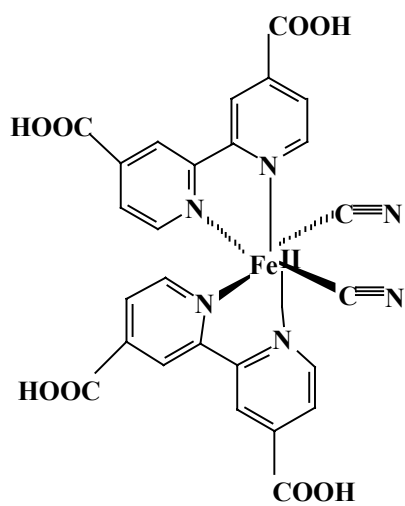


Figure 3: Molecular Structure of  $\text{Fe}^{\text{II}}(4,4'\text{-dicarboxy-2,2'}\text{-bipyridine})_2(\text{CN})_2$ .

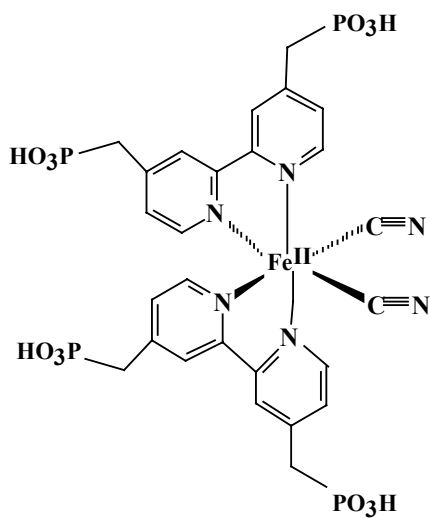


Figure 4: Molecular Structure of  $\text{Fe}^{\text{II}}(4,4'\text{-Bis(methylphosphonate)-2,2'}\text{-bipyridine})_2(\text{CN})_2$ .

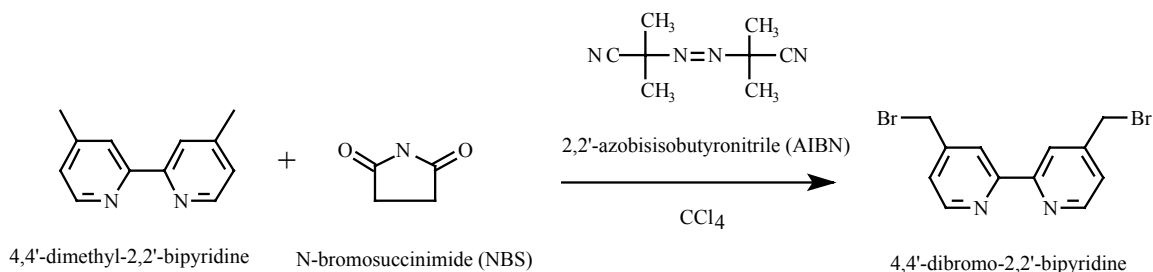


Figure 5: Synthesis of 4,4'-dibromomethyl-2,2'-bipyridine.

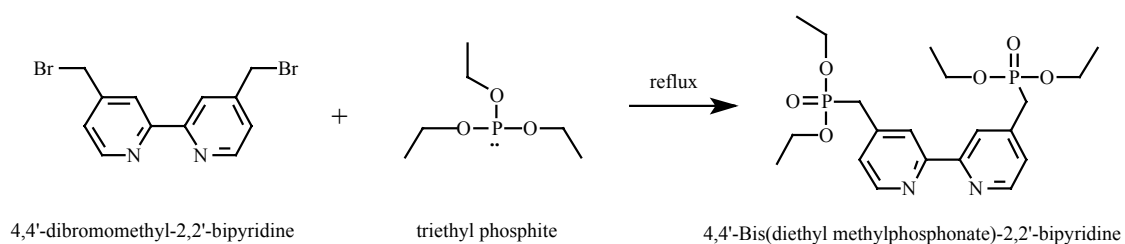


Figure 6: Synthesis of 4,4'-(CH<sub>2</sub>PO(OCH<sub>2</sub>CH<sub>3</sub>)<sub>2</sub>)<sub>2</sub>-2,2'-bipyridine.

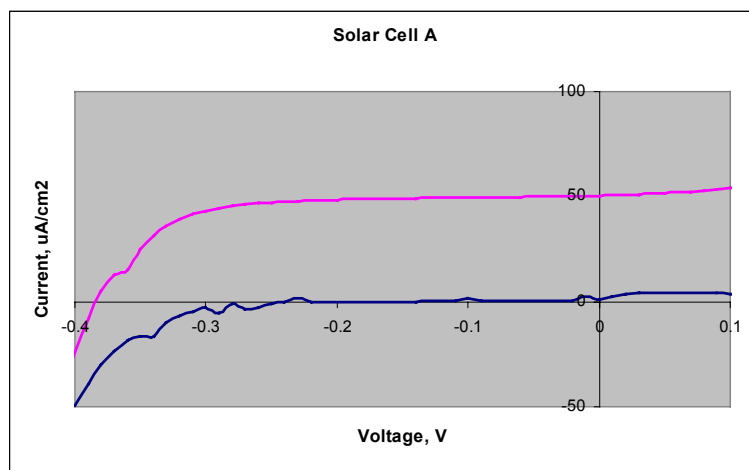


Figure 7A: Current vs Voltage Data for Solar Cell A in .5 M LiI, .5 M I<sub>2</sub> electrolyte solution. Pink is Light Current. Blue is Dark Current.

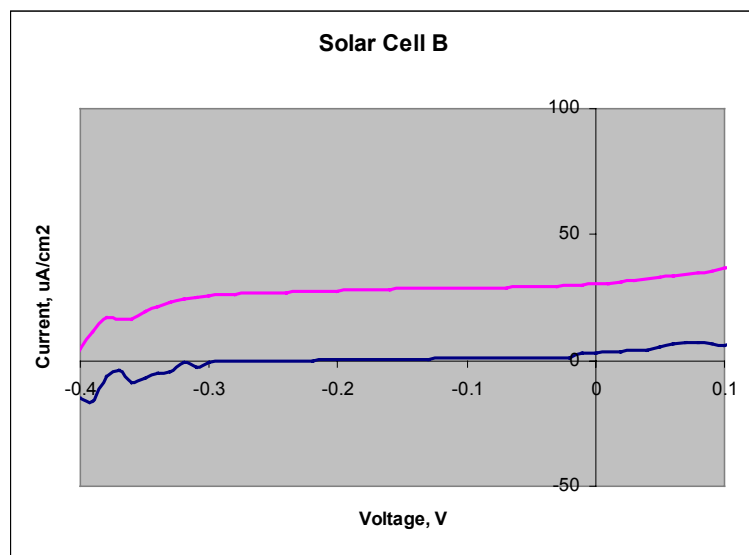


Figure 7B: Current vs Voltage Data for Solar Cell B in .5 M LiI, .5 M I<sub>2</sub> electrolyte solution. Pink is Light Current. Blue is Dark Current.

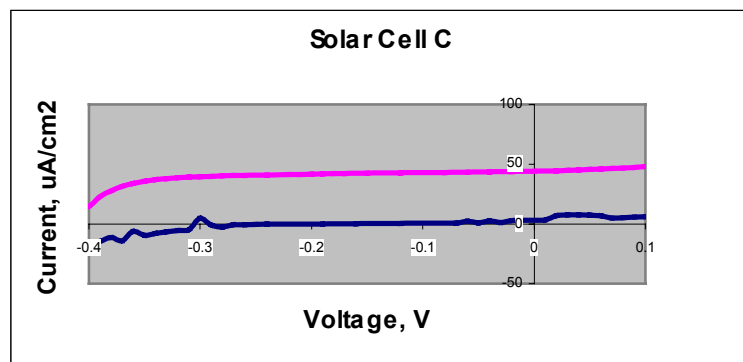


Figure 7C: Current vs Voltage Data for Solar Cell C in .5 M LiI, .5 M I<sub>2</sub> electrolyte solution. Pink is Light Current. Blue is Dark Current.

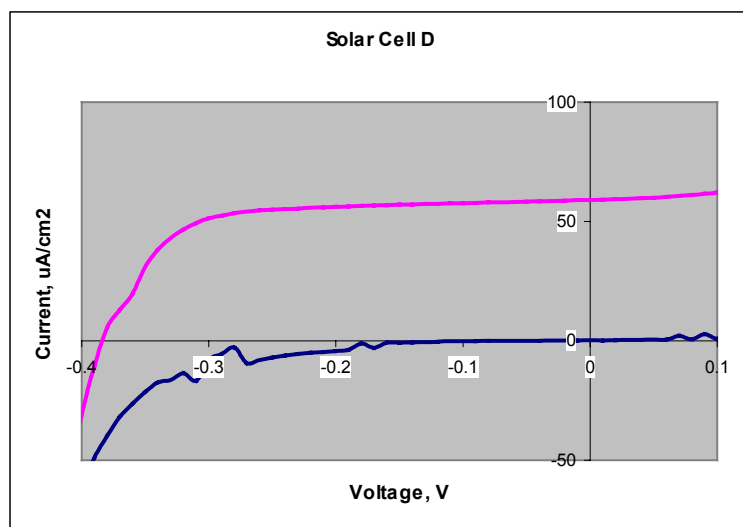


Figure 7D: Current vs Voltage Data for Solar Cell D in .5 M LiI, .5 M I<sub>2</sub> electrolyte solution. Pink is Light Current. Blue is Dark Current.

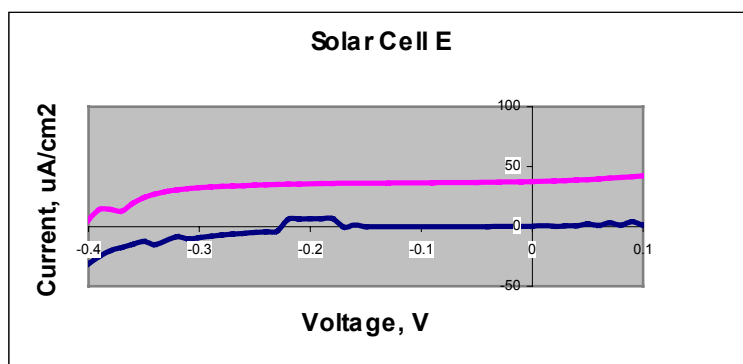


Figure 7E: Current vs Voltage Data for Solar Cell E in .5 M LiI, .5 M I<sub>2</sub> electrolyte solution. Pink is Light Current. Blue is Dark Current.

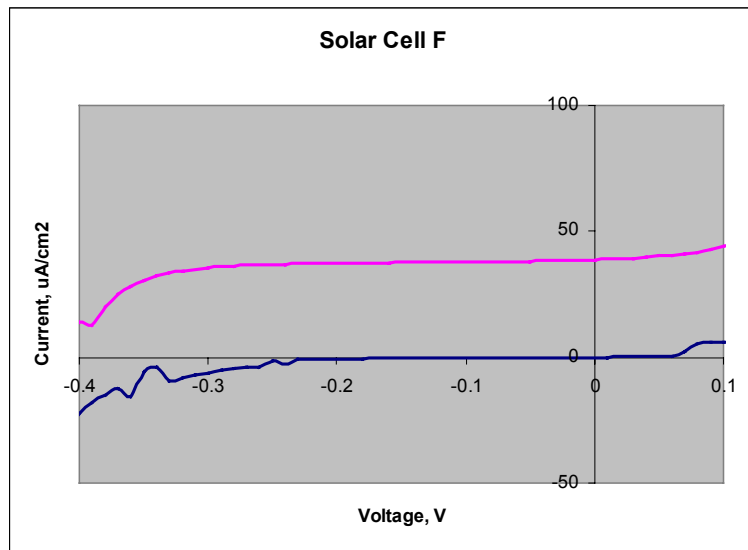


Figure 7F: Current vs Voltage Data for Solar Cell F in .5 M LiI, .5 M I<sub>2</sub> electrolyte solution. Pink is Light Current. Blue is Dark Current.

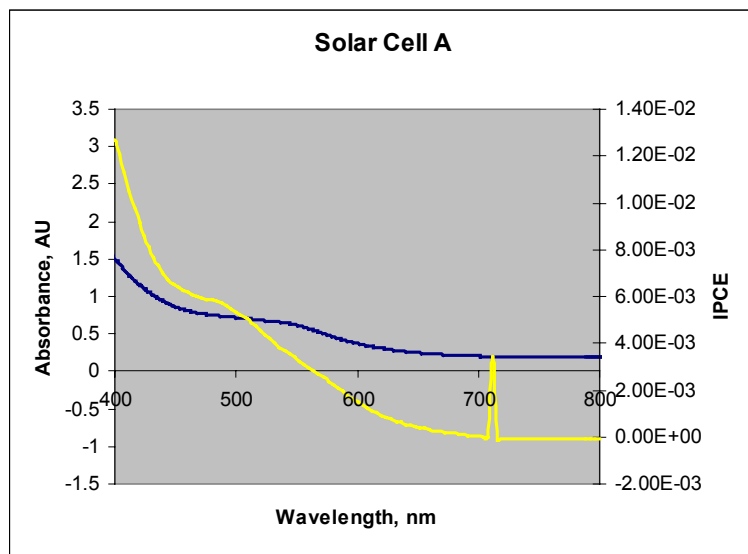


Figure 8A: Absorbance and IPCE Data for Solar Cell A in .5 M LiI, .5 M I<sub>2</sub> electrolyte solution. Blue is Absorbance. Yellow is IPCE.

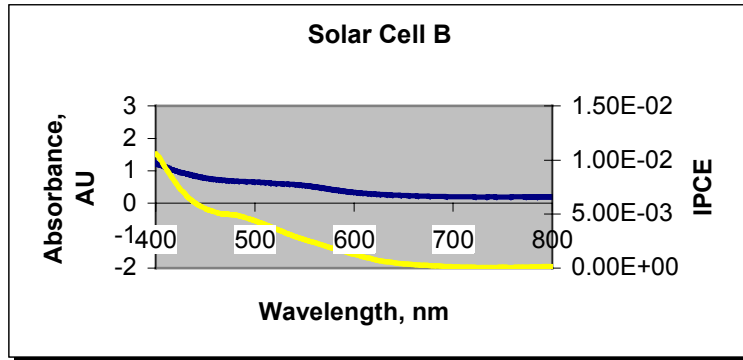


Figure 8B: Absorbance and IPCE Data for Solar Cell B in .5 M LiI, .5 M I<sub>2</sub> electrolyte solution. Blue is Absorbance. Yellow is IPCE.

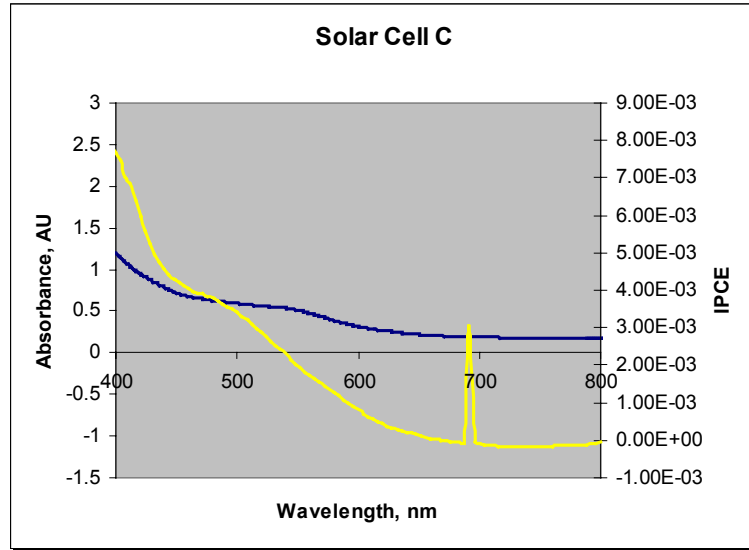


Figure 8C: Absorbance and IPCE Data for Solar Cell C in .5 M LiI, .5 M I<sub>2</sub> electrolyte solution. Blue is Absorbance. Yellow is IPCE.

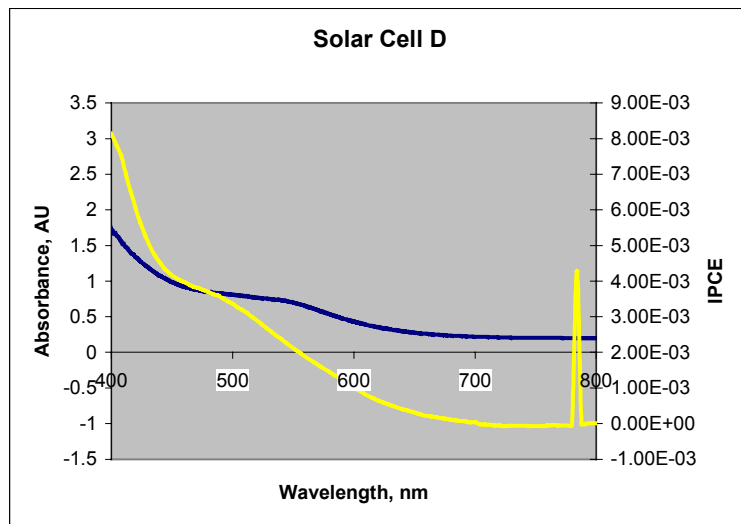


Figure 8D: Absorbance and IPCE Data for Solar Cell D in .5 M LiI, .5 M I<sub>2</sub> electrolyte solution. Blue is Absorbance. Yellow is IPCE.

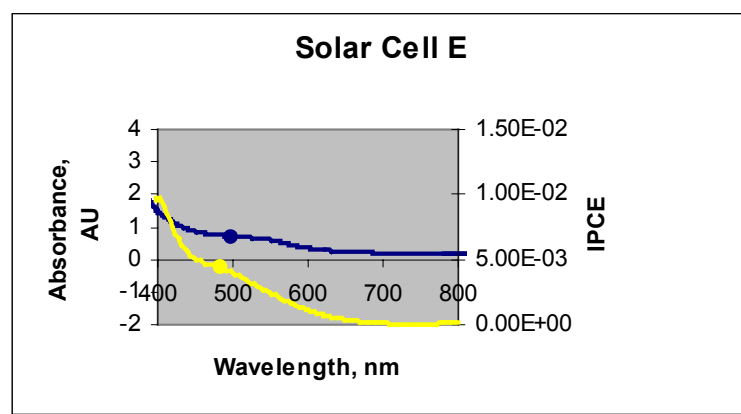


Figure 8E: Absorbance and IPCE Data for Solar Cell E in .5 M LiI, .5 M I<sub>2</sub> electrolyte solution. Blue is Absorbance. Yellow is IPCE.

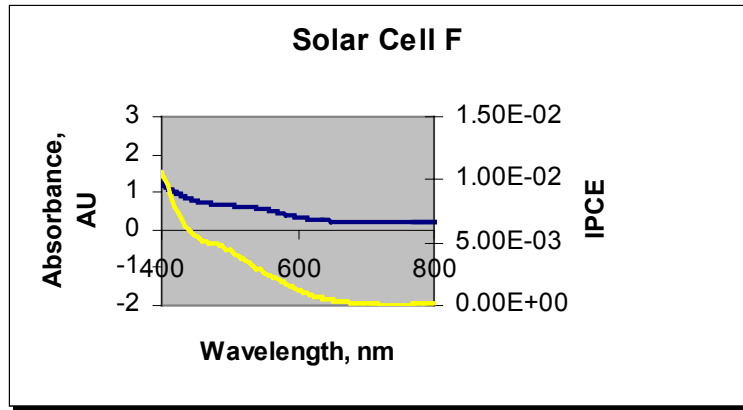


Figure 8F: Absorbance and IPCE Data for Solar Cell F in .5 M LiI, .5 M I<sub>2</sub> electrolyte solution. Blue is Absorbance. Yellow is IPCE.